γ-Ray Strength Functions and GDR Cross Sections in the IAEA Photonuclear Data Project

H. Utsunomiya, I. Gheorghe, D. M. Filipescu, K. Stopani, S. Belyshev, T. Renstrøm, G. M. Tveten, G. Fan, H. Wang, S. Goriely, Y.-W. Lui, T. Ari-izumi, S. Miyamoto, V. Varlamov, B. Ishkhanov, A. C. Larsen, and S. Siem

1 IAEA-CRP F41032

The Coordinated Research Project (CRP) with the code F41032 was launched by the International Atomic Energy Agency (IAEA) in 2016 [1]. The goal of the CRP is to update the photonuclear data library (IAEA-TECDOC-1178) and generate a reference database for photon strength functions. We have been running the PHOENIX Collaboration to acquire new photonuclear data for the IAEA-CRP at the NewSUBARU synchrotron radiation facility in Japan. The collaboration was carried out with the University of Oslo, Extreme Light Infrastructure—Nuclear

H. Utsunomiya (✉) · T. Ari-izumi
Konan University, Kobe, Japan
e-mail: hiro@konan-u.ac.jp

I. Gheorghe · D. M. Filipescu
IFIN-HH, Bucharest-Magurele, Romania

K. Stopani · S. Belyshev · V. Varlamov · B. Ishkhanov
Lomonosov Moscow State University, Moscow, Russia

T. Renstrøm · G. M. Tveten · A. C. Larsen · S. Siem
University of Oslo, Oslo, Norway

G. Fan · H. Wang
Shanghai Advanced Research Institute, Shanghai, China

S. Goriely
Institut d'Astronomie et d'Astrophysique, Université Libre de Bruxelles, Brussels, Belgium

Y.-W. Lui
Texas A&M University, College Station, TX, USA

S. Miyamoto
University of Hyogo, Kobe, Hyogo, Japan

165

Physics (ELI-NP), "Horia Hulubei" National Institute for Physics and Nuclear Engineering (IFIN-HH), Skobeltsyn Institute of Nuclear Physics of Lomonosov Moscow State University (SINP-MSU), and Shanghai Institute of Applied Physics (SINAP). The new data acquired are classified into two groups, (γ, xn) cross section data with $x = 1$–4 for 11 nuclei with 100% natural abundances at γ-ray energies from *1n* threshold up to 40 MeV and (γ, n) cross section data for 21 enriched isotopes at energies below *2n* thresholds. The construction of γSFs was carried out in collaboration with the Université Libre de Bruxelles (ULB).

2 Key Technical Factors

2.1 Laser Compton-Scattering γ-Ray Beam

Quasi-monochromatic pencil-like γ-ray beams are produced in the head-on collision of laser photons from relativistic electrons circulating in the NewSUBARU storage ring. Both INAZUMA (1064 nm) and Talon (532 nm) Q-switch lasers are used to produce quasi-monochromatic pulsed γ-ray beams that are energy-tunable from 4.5 to 76 MeV in collision with electrons from 0.5 to 1.5 GeV. The electron beam is energy-calibrated with the accuracy on the order of 10^{-5} [2]. The electron beam energy is precisely reproduced by the automated control of the beam optics parameters. The γ-ray energy is determined by the calibrated electron beam energy.

The energy profile of the γ-ray beam is determined by reproducing the response function of a 3.5" x 4.0" $LaBr_3(Ce)$ detector to the laser Compton-scattering (LCS) γ-rays with the GEANT4 code which incorporates the kinematics of the LCS process and interactions between the γ-rays and the $LaBr_3(Ce)$ detector. The LCS γ-ray beam is accompanied by a low-energy tail unique to the electron beam emittance and the collimator size. The energy spread for the standard emittance and a collimator of 2 mm aperture located at 18.5 m from the most efficient collision point is typically a few % in the full width at half maximum. The beam size on target approximately follows the geometrical aperture of the collimator with respect to the collision point.

The γ-ray flux is accurately determined from the pile-up/multi-photon spectrum with the Poisson-fitting method [3, 4] based on the fact that the number of photons involved in a γ-pulse follows the Poisson distribution.

2.2 Direct Neutron-Multiplicity Sorting

The Talon laser is operated at 1 kHz to produce a pulsed γ-ray beam that offers 1 ms pulse intervals during which one can identify multi-neutron coincidence events with a moderator-based slow neutron detector. We have developed a neutron detector

consisting of three concentric rings of 4, 9, and 18 ^{3}He counters embedded in a polyethylene moderator at 5.5, 13.0, and 16.0 cm from the γ-ray beam axis [5]. The detector is designed to be of flat response to neutron kinetic energies by tuning the distance and the number of ^{3}He counters for individual rings by GEANT4 simulation. The total detection efficiency is 36.5% with 1.6% uncertainty in one standard deviation over an energy range from 10 keV to 5.0 MeV.

The partial photoneutron cross section with the neutron multiplicity x is determined from the number of reactions (γ, xn) that took place, N_x ($x = 1, 2, 3,..$), in an experiment. However, the number of reactions is not a direct experimental observable. Instead, the number of neutron coincidence events is the experimental observable. In general, a moderator-based neutron detector has a strong dependence of the detection efficiency on neutron kinetic energy. In this case, the ring-ratio technique which was originally developed by the Lawrence Livermore National Laboratory [6] cannot determine the average neutron kinetic energy for the individual (γ, xn) reactions. In view of the fact that the neutron kinetic energy is different in (γ, xn) reactions with a different x and in the emission order of neutrons in the same (γ, xn) reactions, one encounters a difficulty in neutron-multiplicity sorting with the ring-ratio technique.

The best way for overcoming the difficulty is to utilize a flat-efficiency detector to determine the number of reactions N_x by solving a set of equations for the experimental observables, the number of neutron coincidence events. One can refer to Ref. [5] for details of the direct neutron-multiplicity sorting with a flat-efficiency detector.

3 Data Acquisition, Evaluation, and Compilation

We have successfully acquired all the data as originally time-scheduled as follows. The institute which is responsible for the data reduction of (γ, xn) cross sections is shown in the parentheses. The data reduction of (γ, n) cross sections is undertaken by the University of Oslo.

I. (γ, xn) data on 11 nuclei
  2015: ^{9}Be(Konan), ^{208}Bi(ELI-NP/IFIN-HH)
  2016: ^{89}Y(SINP-MSU), ^{169}Tm(ELI-NP/IFIN-HH), ^{197}Au(Konan)
  2017: ^{59}Co(SINP-MSU), ^{165}Ho(ELI-NP/IFIN-HH), ^{181}Ta(Konan)
  2018: ^{103}Rh(SINP-MSU), ^{139}La(Konan), ^{159}Tb(ELI-NP/IFIN-HH)
II. (γ. n) data on 21 nuclei
  2015: ^{89}Y, ^{203}Tl, ^{205}Tl
  2016: ^{13}C, ^{58}Ni, ^{60}Ni, ^{61}Ni, ^{64}Ni, ^{137}Ba, ^{138}Ba, ^{185}Re, ^{192}Os
  2017: ^{64}Zn, ^{66}Zn, ^{68}Zn, ^{182}W, ^{183}W, ^{184}W
  2018: ^{156}Gd, ^{157}Gd, ^{158}Gd, ^{160}Gd

The data newly acquired in the PHOENIX Collaboration are evaluated by the Japan Atomic Energy Agency (JAEA), the Chinese Nuclear Data Center (CNDC), and Korean Atomic Energy Research Institute (KAERI) and compiled in the IAEA updated photonuclear data library. The data are also used to supplement the (γ, γ') and the Oslo method data to construct the photon strength function and compiled in the IAEA reference database for photon strength functions.

4 γ-Ray Strength Function

Figure 1 shows the γ-ray strength function (γSF) for Ni isotopes constructed with the γSF method [7] which has been devised to investigate systematically (γ, n) and (n, γ) cross sections over an isotopic chain. The present (γ, n) data are used as experimental constraints on the model E1 and M1 γSFs from the Hartree–Fock–Bogolyubov plus quasi-particle random phase approximation based on the Gogny D1M interaction. The recent systematics of the γSF [8] has been taken into account; the γSF in de-excitation mode differs from that in excitation mode in the zero-limit behavior of both E1 and M1 strengths, the latter of which is referred to as M1 upbend. In the figure, the M1 γSF is shown for two different zero-limit values, 3×10^{-8} and 10^{-7} MeV^{-3}.

The mean field plus QRPA calculations need some phenomenological corrections, which include a broadening of the QRPA strength to take the neglected damping of collective motions into account as well as a shift of the strength to lower energies due to the contribution beyond the one-particle–one-hole excitations and the interaction between the single particle and low-lying collective phonon degrees of freedom. As such phenomenological corrections [8], we have introduced an E1 damping width of 4.5 MeV which is smaller than the systematics of $\Gamma_{E1} = 7 - A/45$ MeV [8] due to the closed proton shell in Ni isotope and M1 damping width of 2 MeV. As a consequence, a factor of 2/3 on the overall E1 strength is required to reproduce the present peak photoneutron cross section in the GDR region. More details can be found in Ref. [7].

5 GDR Cross Section

5.1 ^{209}Bi

Previously we published GDR cross sections for ^{209}Bi [12]. We found it necessary to take into account the effect of the electromagnetic interaction (pair production, Compton scattering, and photoelectric absorption) of high-energy γ-ray beams in the thick (7 mm or 10 mm) ^{209}Bi target material on the (γ, xn) cross sections [13]. The interaction produces the secondary gamma rays which can induce the giant
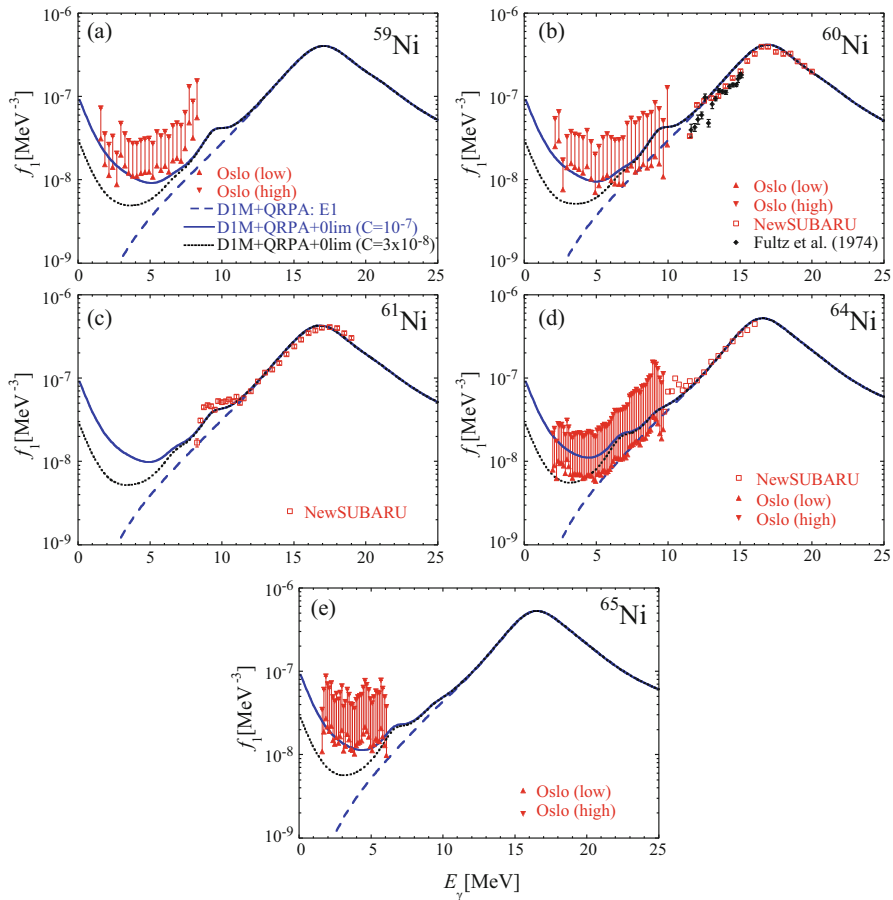
Fig. 1 (**a**)–(**e**) γSF for the ^{59,60,61,64,65}Ni isotopes. The red triangles correspond to the upper and lower limits of the γSF extracted from the Oslo data and the red open squares to the NewSUBARU photoneutron data. The dashed blue curve represents the D1M + QRPA E1 strength and the black dotted (blue full) line the D1M + QRPA +0lim E1 + M1 dipole strength obtained with $C = 3 \times 10^{-8}$ MeV^{-3} ($C = 10^{-7}$ MeV^{-3}). The γSF of ^{64,65}Ni is taken from Refs. [9, 10] (red triangles). The γSF extracted from the ^{60}Ni(γ,n) data of Fultz et al. [11] (black diamonds) is also shown in panel (**b**)

dipole resonance most effectively in the peak region around 13 MeV governed by the (γ, n) channel. Thus, the secondary gamma rays produce extra neutrons which we previously assigned to reaction neutrons of the (γ, n) channel associated with the primary gamma rays. We have corrected the (γ, xn) cross section for the effect. As a result, the (γ, n) cross section is significantly reduced above 30 MeV, while the (γ, xn) cross section with x = 2–4 remains the same.

Fig. 2 (Color online)
Comparison of the revised
total experimental cross
section with the TALYS
predictions for two values of
the Levinger parameter
$L = 6.5$ (solid line) and
$L = 20$ (dashed line)
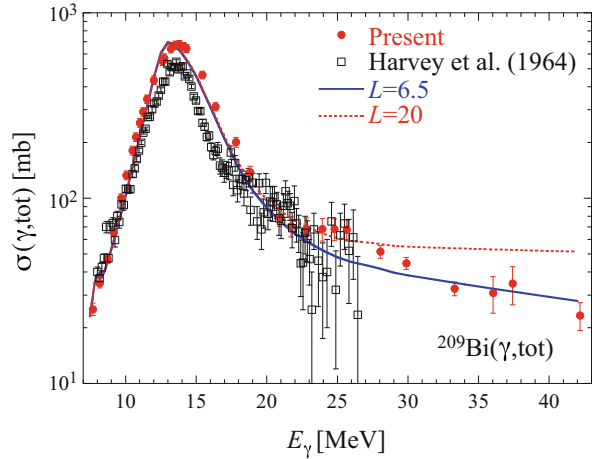
Here, we show the total photoneutron cross section in Fig. 2, leaving details on partial photoneutron cross sections in Ref. [13]. The asymptotic value of the total cross section is reproduced by the default pre-equilibrium calculation with an ordinary value ($L = 6.5$) of the Levinger parameter for the quasi-deuteron contribution. Previously we discussed the large cross section at the high energies in terms of an increase of the L value and the surface effect. With the corrected cross sections, however, there is no need to require a large value $L = 20$ nor to invoke the surface effect anymore.

5.2 ^{159}Tb

Figure 3 shows partial photoneutron cross sections (γ, xn) with $x = 1$ and 2 for ^{159}Tb. The ^{159}Tb is one of 19 nuclei for which the Livermore and Saclay data of partial photoneutron cross sections show serious discrepancies [14]. One can see that the present (γ, n) cross section is rather consistent with the Saclay data, while the (γ, $2n$) cross section agrees with the Livermore data.
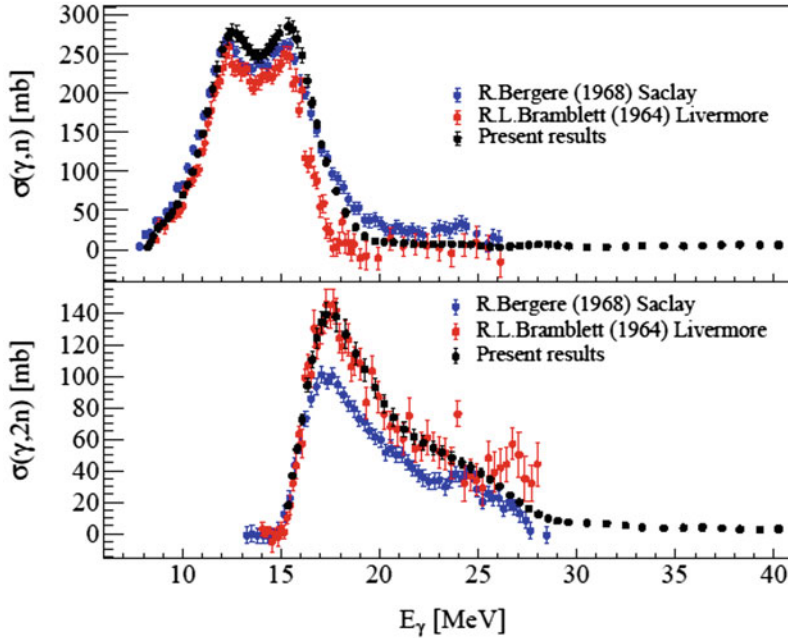
Fig. 3 Partial cross sections (γ, xn) with $x = 1$ and 2 for ^{159}Tb in comparison with the Livermore [15] and Saclay [16] data

6 Summary

We have made an intensive effort of measuring (γ, n) and GDR cross sections within the framework of the international PHOENIX Collaboration for the IAEA-CRP F41032 on creating compilations of photonuclear reactions and photon strength functions. The two compilations have been published in 2019 [17] and 2020 [18], respectively, followed by publications of the individual photonuclear data in the context of nuclear reaction and structure in nuclear physics and nucleosynthesis of heavy elements in nuclear astrophysics.

References

1. P. Dimitriou et al., EPJ Web of Conf. **93**, 06004 (2015)
2. H. Utsunomiya et al., IEEE Trans. Nucl. Sci. **61**, 1252 (2014)
3. T. Kondo et al., Nucl. Instrum. Methods A **659**, 462 (2011)
4. H. Utsunomiya et al., Nucl. Instrum. Methods A **896**, 103 (2018)
5. H. Utsunomiya et al., Nucl. Instrum. Methods A **871**, 135 (2017)
6. S.C. Fultz et al., Phys. Rev. **162**, 1098 (1967)
7. H. Utsunomiya et al., Phys. Rev. C **98**, 054619 (2018)
8. S. Goriely, S. Hilaire, S. Péru, K. Sieja, Phys. Rev. C **98**, 014327 (2018)
9. L. Crespo Campo et al., Phys. Rev. C **94**, 044321 (2016)

10. L. Crespo Campo et al., Phys. Rev. C **96**, 014312 (2017)
11. S.C. Fultz, R.A. Alvarez, B.L. Berman, P. Meyer, Phys. Rev. C **10**, 608 (1974)
12. I. Gheorghe et al., Phys. Rev. C **96**, 044604 (2017)
13. I. Gheorghe et al., Phys. Rev. C **059901**(E), 99 (2019)
14. V.V. Varlamov et al., Eur. Phys. J. A **50**, 114 (2014)
15. R.L. Bramblett et al., Phys. Rev. **133**, B869 (1964)
16. R. Bergere, H. Beil, A. Veyssiere, Nucl. Phys. A **121**, 463 (1968)
17. S. Goriely *et al.*, Eur. Phys. J. A **55**, 172 (2019)
18. T. Kawano *et al.*, Nuclear Data Sheets **163**, 109 (2020)